We are IntechOpen, the world's leading publisher of Open Access books Built by scientists, for scientists

4,800
Open access books available

122,000
International authors and editors

135M
Downloads

Our authors are among the

154
Countries delivered to

TOP 1%
most cited scientists

12.2%
Contributors from top 500 universities

WEB OF SCIENCE™

Selection of our books indexed in the Book Citation Index in Web of Science™ Core Collection (BKCI)

Interested in publishing with us?
Contact book.department@intechopen.com

Numbers displayed above are based on latest data collected.
For more information visit www.intechopen.com

Chapter 15

Computational Dynamics of Anti-Corrosion Performance of Laser Alloyed Metallic Materials

Olawale S. Fatoba, Patricia A.I. Popoola, Sisa L. Pityana and Olanrewaju S. Adesina

Additional information is available at the end of the chapter

http://dx.doi.org/10.5772/62334

Abstract

Laser surface alloying (LSA) is a material processing technique that utilizes the high power density available from defocused laser beam to melt both reinforcement powders and a part of the underlying substrate. Because melting occurs solitary at the surface, large temperature gradients exist across the boundary between the underlying solid substrate and the melted surface region, which results in rapid self-quenching and resolidifications. Reinforcement powders are deposited in the molten pool of the substrate to produce corrosion-resistant coatings. These processes influence the structure and properties of the alloyed region. A 3D mathematical model is developed to obtain insights on the behavior of laser melted pools subjected to various process parameters. It is expected that the melt pool flow, thermal and solidification characteristics will have a profound effect on the microstructure of the solidified region.

Keywords: Laser Process Parameters, Computational Dynamics, Anti-Corrosion Performance, Martensitic stainless steels, Mild steel

1. Introduction

1.1. Laser surface treatment

Laser surface treatment has a strong impact on classical manufacturing and repair tasks, addressing markets such as turbo machinery, aeronautics, automotive, off-shore and mining as well as tool, die, and mould making and life science [1]. According to Steen and Mazumdar [2], laser has some distinctive properties for surface heating. For opaque materials, such as metals, the laser beam electromagnetic radiation is absorbed within the first few atomic layers and there are no associated eddy currents or hot gas jets. Moreover, there is no radiation spillage

outside the optically defined beam area. Compared with other methods of surface modification, laser surface engineering is characterized by possibility of forming alloys of non-equilibrium compositions, formation of a fine microstructure, development of a metallurgical bond between the surface layer and the substrate, a small heat-affected zone and the combination of a controlled minimal dilution of the substrate by the coating material, and nevertheless, a very strong fusion bond between them. Characteristics and advantages such as high productivity, automation worthiness, non-contact processing, elimination of finishing operation, reduced processing cost, improved product quality, greater material utilization and minimum heat affected zone have led to increasing demand of laser in material processing [3–5].

1.2. Categories of lasers

Lasers can be classified according to their active medium, wavelength, and excitation mechanism. There are various types of lasers used in industries, but the common type of lasers used are gas, solid-state, dye, and diode lasers also known as semiconductor lasers classified according to their active medium.

1.2.1. Gas lasers

Gas lasers utilize gas or gas mixture as their active medium. Excitation usually is achieved by current flow through the gas. During operation, the gas is often in the state of plasma, containing a significant concentration of electrically charged particles. Frequently used gases include CO_2, argon, krypton, excimer, and gas mixtures such as helium–neon. The most commonly used gas laser in materials processing is the CO_2 laser. CO_2 lasers use a gas mixture of CO_2, helium (He), nitrogen (N_2), and possibly some hydrogen (H_2), water vapor, and/or xenon (Xe) for generating laser radiation. CO_2 lasers emit light with a wavelength of 10.6 μm with an overall efficiency of 10–13%. Regardless of the low efficiency, the CO_2 lasers have a good beam quality and focusability. They are widely used in engineering and material processing because of the high power that can be obtained (>5 kW) and the high speed accuracy for cutting, welding, and marking both ferrous and non-ferrous materials.

1.2.2. Solid-state lasers

Solid-state lasers, also called solid crystalline or glass lasers, consist of a host and an active ion doped in the solid host material. The active media used are rare earth ions such as neodymium, erbium, and holmium and transition metals such as chromium, titanium, nickel, and others. The most common utilized ions are Cr^{3+} and Nd^{3+} with the host as yttrium aluminum garnet (YAG), glass, and yttrium lithium fluoride (YLF). The beam has a wavelength of 1.06 μm. These lasers generate high output powers, or lower powers with very high beam quality, spectral purity, and stability. These lasers have found major applications in the automotive industry for its high speed welding of body components [6].

1.2.3. Diode lasers

Diode lasers, also known as semiconductor lasers, are based on semiconductor grain media, which are diodes that are electrically pumped. They operate based on electrical pumping with

http://dx.doi.org/10.5772/62334

moderate voltages. High efficiency can be achieved particularly for high-power diode lasers and allows their use as pump sources for highly efficient solid-state lasers and diode-pumped lasers. Diode lasers are much smaller than gas or solid state lasers in the same power range. They have found major success in conduction welding, cladding, and laser hardening. Their applications are extremely widespread, including areas as diverse as optical data transmission, optical data storage, metrology, spectroscopy, and materials processing.

1.2.4. Dye lasers

Dye lasers use an organic dye as the gain medium with gain spectrum as available dye or a mixture of dyes. Dye lasers are normally pumped at short wavelengths with a green laser such as argon ion laser, a frequency doubled solid state laser, or an excimer laser emitting ultraviolet light. The most important feature in dye lasers is the output wavelength that can be adjusted. Today, they are still used in areas such as spectroscopy for chemical analysis of gaseous samples because of their distinct wavelengths that are hard to generate [7].

1.2.5. Fiber lasers

Fiber lasers belong to the solid-state laser group. Laser beams are generated by means of seed laser and magnified in specially designed glass fibers, which are supplied with energy through pump diodes. Fiber lasers with a wavelength of 1.064 μm produce an exceedingly small focal diameter; consequently, their intensity is up to 100 times higher than that of CO_2 lasers with the same emitted average power. Fiber lasers are optimally suited for metal marking via annealing, for high-contrast plastic markings, and for metal engraving. Fibers feature a long service life of at least 25,000 laser hours and are generally maintenance free.

1.3. Industrial applications of different lasers

Lasers are preferable tools compared with the other traditional ones. They are widely used in industry for cutting, welding, surface treatments, and drilling, especially in the automobile industry in developed countries [8–10]. Most car frames are produced by laser cutting on a programmed robot assembly line. Also many car components are laser treated or processed. Moreover, lasers are also functionally used for medical purposes such as short-sight correction and cancer operations. Other applications such as those used for communications, data transmission, internet backbones, and audio vision home appliances are increasingly used in daily life. Table 1 shows industrial application of different lasers.

1.4. Laser surface modification techniques

Laser surface techniques have attracted industries owing to the possibility of accurate control of the area where laser radiation is delivered, as well as the amount and rate of energy deposition. The flexibility of control of the beam's interaction with regard to wavelength, energy density, and interaction time and the wide choice of interacting environments has led to the significant developments in laser technology such as laser welding, drilling, alloying, and cladding [11]. The laser's ease of automation and robotic manipulation capability also

Type of laser	Wavelength	Areas of application
Carbon dioxide (CO_2)	10.6 μm	Material processing, surgery, etc.
Dye laser	390–640 nm	Medicine, birth mark removal
Nd: YAG	1.064 μm	Material processing
Nd: Glass	1.062 μm	Velocity and length measurement
Excimer	193 nm	Laser surgery
Ruby	694.3 nm	Tattoo removal, holography
Hydrogen fluoride	2.7–2.9 μm	Laser weapon
Helium-neon	632 nm	Holography, spectroscopy
Argon	454.6 nm	Lithography, spectroscopy

Table 1. Industrial applications of different lasers

make laser surface technique very suitable for repair activities in extreme or remote environments, such as under water or in areas with radioactive contamination [12].

The distinctive advantages of the laser surface alloying (LSA) technique for surface modification include the refinement of the grain size because of rapid quench rates and the generation of meta-stable structures with novel properties that are not feasible by competing methods and laser surface alloying (LSA) modifies the surface morphology and near surface structure of components and its alloys with perfect adhesion to the interface of the bulk steel [13,14]. With optimal laser processing parameters, a dependable coating that is free of pores and cracks can be produced on the matrix. LSA can rapidly provide a crack-free and thick layer in all instances with metallurgical bonds at the boundary between the substrate and alloyed layer [15]. In LSA, external alloying elements in the form of powder, paste, suspension, electrolytic coatings, and plasma or flame sprayed coatings are introduced into the surface of a substrate, as preplaced addition material or injected directly into the melt pool, treated by a high power laser beam [16]. The particles introduced in the interaction zone completely dissolve in the liquid phase, thereby modifying the surface layer chemical composition [17,18]. The result of this is a rapid self quenching and resolidification of new alloy because of the large temperature gradients between the substrate and melted surface region [6]. Evolution of a wide variety of microstructures is one of the consequences as a result of the rapid cooling from the liquid phase [19,20]. Hence, the synthesis of new alloy is possible by depositing a premixed ratio of elemental powders during laser alloying. Powders alloyed on worn or new working surfaces of components by LSA provide specific properties such as erosion resistance, corrosion resistance, high abrasive wear resistance, heat resistance, and combinations of these properties. Consequently, safety in automotive and aerospace applications and improvements in machinery performance can be realized by the method [21]. According to Poulon-Quintina et al. [22], laser beams can generate specific microstructures including nanocrystalline grains and metastable phases because of specific thermal characteristics induced by laser irradiation. Laser processing offers cost advantages and exceptional and important quality over traditional

http://dx.doi.org/10.5772/62334

techniques. These include process compactibility, low porosity, high throughput speed, high process efficiency, and good surface homogeneity; in addition, the formation of a amorphous or non-equilibrium phase as well as refinement and homogenization of the microstructure, all without affecting the bulk properties of the substrate [23,24] as shown in Figure 1.

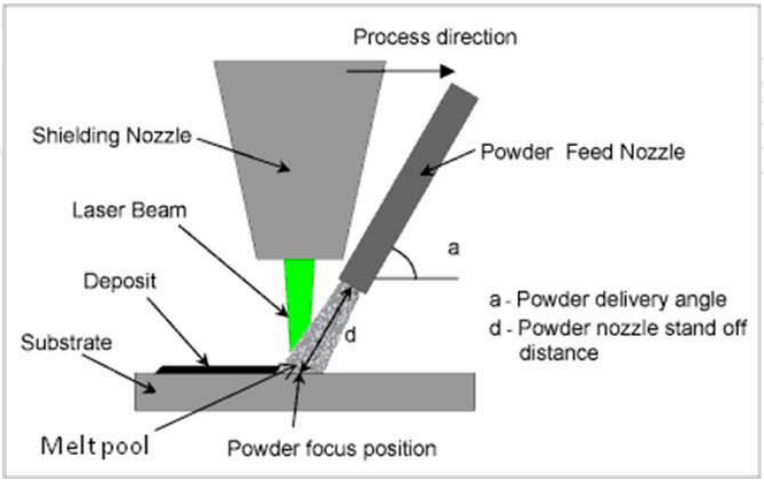

Figure 1. Schematic diagram of laser alloying experimental process (www.twi-global.com).

1.5. Laser beam characteristics

Laser beam characteristics play a very important role in laser material processing. Laser beam is characterized by several parameters such as laser beam mode, focusability, and polarization. The beam with low divergence angle produces a smaller focused spot and greater depth of focus [25]. The laser energy can be distributed in a uniform or Gaussian distribution over the laser beam spot area. To achieve a good quality beam, it is necessary to resonate the beam in a chamber where certain distributions of amplitude and phases of electromagnetic field can be produced because of repeated reflections between the mirrors [26]. These specific shapes produced in the resonator are called transverse electromagnetic modes (TEMs). Each TEM is a different energy distribution across the beam. TEM_{00} (Gaussian) and TEM_{01*} (created by oscillation between orthogonal TEM_{01} modes) are common in industrial lasers.

Another important issue is the reflectivity from the surface of the metal. The reflectivity is a strong function of laser wavelength and temperature, and it varies from metal to metal. As the temperature increases in the process zone, reflectivity decreases and absorptivity increases because of an increase in the photon population [27], and this indicates the potential for more energy absorption by hot material. However, this is only true when the surface conditions remain constant. In practice, there is often oxidation or phase change, which can alter this behavior of absorptivity. Laser absorption differs from one material to the other based on the wavelength of the laser. For example, CO_2 laser is very well absorbed in plastics and plywood, whereas Nd:YAG is poorly absorbed in the same materials. Nd:YAG has good absorption in steel and non-ferrous metals, whereas CO_2 laser is poorly absorbed in some non-ferrous metals [28]. Some metals and their absorptivity in different lasers are shown in Figure 2.

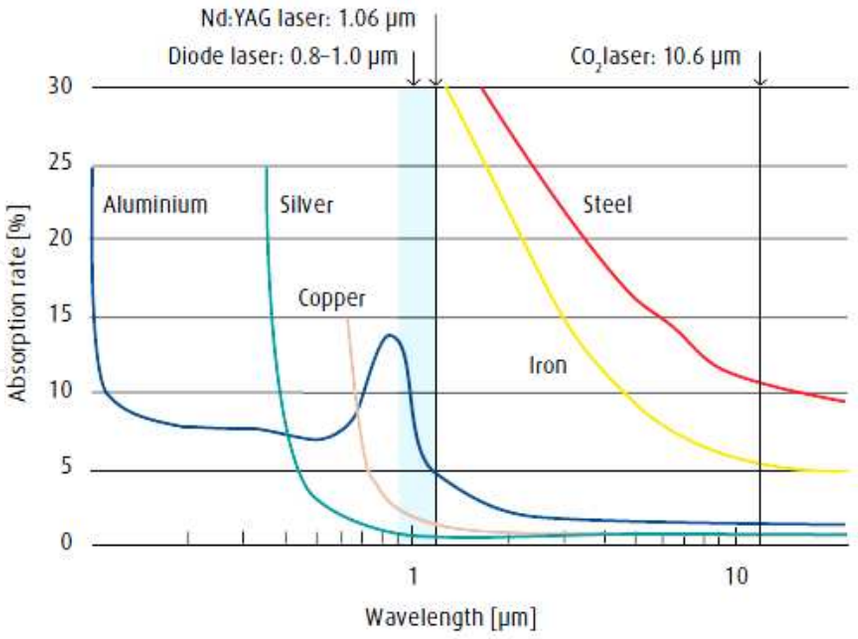

Figure 2. Absorption rate of laser radiations in cold metal [28].

2. Mechanism of heat transfer in laser processing

Heat is defined as energy transferred by virtue of a temperature difference. It flows from a high temperature region to a low temperature region. Heat transfer is used to predict the energy transfer taking place in the material bodies, which result from the temperature difference. There are three modes of heat transfer: conduction, convection, and radiation [29–32].

2.1. Conduction heat transfer

Conduction is transfer of the energy from high temperature region to the low temperature region in a body. In this situation, a temperature gradient will be formed, and heat is transferred by conduction. The rate of heat transfer per unit area is proportional to the normal temperature gradient:

$$q = -KA\frac{\partial T}{\partial x} \tag{1}$$

This is called Fourier's law of heat conduction. The positive constant K is the thermal conductivity of the material. The negative sign is included to ensure that heat flows in the direction of decreased temperature. q is the rate of heat transfer and $\frac{\partial T}{\partial x}$ is the temperature gradient in the direction of the heat flow. The unit of thermal conductivity K is $W/m/K$. Similarly, heat

http://dx.doi.org/10.5772/62334

conduction rate equation can be written in y and z directions. In general, the heat flux is a vector quantity and is expressed as follows:

$$\vec{q} = -k\nabla T \tag{2}$$

$\bar{q}$ = Local heat flux density, W/m^2

k = Thermal conductivity of material, $W/m/k$

∇T = Temperature gradient, K/m

2.2. Convection heat transfer

Convection heat transfer is related to the transfer of heat from a bounding surface to a fluid in motion, or to the heat transfer across a flow plane within the interior of the flowing fluid. If the fluid motion is induced by the fan, blower, pump, or some other similar device, the process is called forced convection. If the fluid motion occurs as a result of the density difference produced by the temperature difference, the process is called free or natural convection [33]. The velocity of the fluid motion obviously influences the heat-transfer rate. Thus, the defining equation of convection heat transfer is:

$$q = hA(T_w - T_\infty) \tag{3}$$

The symbol h is called the convection heat-transfer coefficient. An analytical calculation of h may be made for some systems, but for complex situations it must be determined experimentally. The units of convection heat-transfer coefficient h are in watts per square meter per Celsius degree when the heat flow is in watts. Convection heat transfer will have a dependence on the viscosity of the fluid in addition to its dependence on the thermal properties of the fluid (e.g., thermal conductivity, specific heat, density).

2.3. Radiation heat transfer

In the conduction and convection heat transfer system, the energy is transferred through a material medium. However, in the radiation heat transfer system, heat energy can be transferred through the perfect vacuum regions. The mechanism involved is electromagnetic radiation that is propagated as a result of a temperature difference, which is called thermal radiation. Thermal radiation is electromagnetic radiation emitted by a body by virtue of its temperature and at the expense of its internal energy. Thermal radiation has same nature to the visible light, x-rays, and audio waves. The differences between these are their wavelengths and the source of generation. From thermodynamic consideration, an ideal thermal radiator or blackbody that emits energy, its rate is proportional to the fourth power of the absolute temperature of the body and directly proportional to its surface area. Thus,

$$q_{\text{emitted}} = \sigma A T^4 \tag{4}$$

q = Heat transfer per unit time (W)

σ = 5.669 × 10^{-8} W/m^2K^4

T = Absolute temperature, Kelvin (K)

This equation is the Stefan-Boltzmann law of thermal radiation. It governs only radiation emitted by a blackbody [33]. The equation is valid only for thermal radiation and may not be treated for other types of electromagnetic radiation so simply. Letter σ is the proportionality constant and is called the Stefan-Boltzmann constant with the value of 5.669 × 10^{-8} W/m^2K^4.

3. Mechanism of laser surface alloying

A focused laser beam as a heat source is used by laser alloying to create a melt pool on an underlying substrate. Powder material is then deposited through the nozzles into the melt pool. The deposited powder is then bonded with the substrate upon solidification. Laser alloying is a process similar to cladding except that another component of the alloy is injected into the molten pool of substrate. Alloying requires a greater laser power density than cladding [8]. The alloying process enables metallic and ceramic alloys [8] to be obtained. The process starts with melting of a substrate by laser irradiation. On the surface of a melt, there is temperature distribution, T, which results in the surface tension distribution, γ, as shown in Figure 3. The convection movement of the melt pool is caused by the surface tension, which pulls the materials from the center. When solid particles are injected into the melt pool, there is a good mixing of the particles with the substrate material. Melting of the particles and reaction with the substrate can then take place. As the laser beam moves to the next position, the reaction slows down and stops. Metastable phases are formed as a result of the subsequent rapid cooling of the melt. However, lowering the speed of the laser beam can also slow down the rate of cooling.

Solidification of remelted materials and convection motions in the laser melt pool decide the final distribution of the alloying element in the remelted zone and a big temperature gradient. The powder is either introduced directly by the nozzle during alloying or applied as paste that dries up on the specimen surface, and then subjected to alloying. This makes it possible to develop an alloy with bi- or multi-component structure. Moreover, a high degree of adhesion is obtained between the substrate and the coating, and the rapid self cooling made possible by heat removal to the cold substrate is responsible for the development of advantageous, fine-grained, and novel microstructures [34–36].

Figure 3 shows a schematic diagram of a typical laser surface alloying process. As shown in the figure, a part of the energy is absorbed when a laser beam with defined power moves with a steady scanning speed in a parallel direction and strikes the surface of a solid material. A melt pool is formed on the surface because of laser heating. Concurrently, particles fed into

http://dx.doi.org/10.5772/62334

the melt pool mixes with the molten substrate by convention and diffusion. Resolidification and several complex phenomena of the region occur, as the laser beam moves away from one position to another, leading to a final microstructure of the alloyed surface.

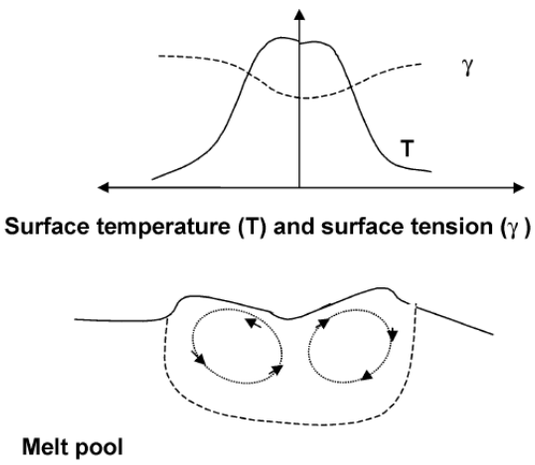

Figure 3. Surface temperature (T) and surface tension (γ) distribution across a laser melted pool [37].

4. Transport phenomena in laser alloying process

The characteristics of the molten pool were studied through experimental investigation and numerical modeling by Yang et al. [38]. The authors reported that the Marangoni flow takes hot fluid from the free surface toward the bottom of the melt pool. Likewise, Sarkar et al. [39] also studied heat, momentum, and mass transfer in a laser alloying process. The authors reported that concentration of particles in the molten pool could be predicted. Raj et al [40] reported that the melting of particles injected into the molten pool is not instant and the particles' mass flux boundary condition is difficult to model. Chung and Das [41] studied laser-induced vaporization, melting, and resolidification in metals. The authors derived the relationship for the times needed to commence melting, attain vaporization, and reach the maximum melting depth during the laser heating pulse. Li et al. [42] showed that the model integrating the volumetric heating source is more exact in the prediction of the melting process than the model of the surface heating source. Safdar et al. [43] investigated the geometry of the laser beam influence on the laser transformation hardening of steel. The authors found out that the best thermal history was produced by the triangular beam geometry in other to achieve improved highest hardness and transformation hardening without sacrificing the hardening depths and processing rate. Authors [44–47] studied surface tension gradient's imposition on the characteristics of the convention. However, several essential aspects still remain inexplicable. Among them are the instability of microflows and mechanisms of capillary thermal-concentration convection manifestation [44,45]. The thermal-capillary convection also known as Marangoni convection is one of the overriding factors dictating the quality of the laser alloying.

There are three important physical processes such as mass transfer, heat transfer, and convection transfer in laser molten pool. The rate of heating and cooling is determined by energy transfer, whereas the extent of mixing and final composition is determined by the convection and mass transfer. Specifically, convection transfer in laser molten pool can strongly affect the quality of laser alloying, cladding, and welding. Some computer simulations of heat and mass transfer have been reported [36,48]. To study the mechanism of convection in theory, 3D computer simulation of convection and heat transfer in laser molten pool are needed. The main physical process in laser molten pool requires some of the laser beam to be absorbed while the rest is reflected. If the threshold is exceeded by the heat absorbed, the molten pool will be developed. In stationary melting, molten pool shape and absorbability are constant. The buoyancy force and the surface tension gradient are the two driving forces for fluid flow in laser melt pool.

Safdar et al. [43] studied the effects of non-conventional laser beam geometries on the melting of metallic materials. The authors reported that the laser beam geometries did not have a significant effect on the resulting melt characteristics because of the high thermal conductivity of metals. Laser power intensity was the most significant processing parameter on the phase change in the irradiated region studied by Konrad et al. [49] when melting of a subcooled metal particle was subjected to a nanosecond laser heating. Bin-Mansoor and Yilbas [50] studied the laser heating and the phase change process in the irradiated region. However, the studies were limited to either two-dimensional axi-symmetric heating situations or moving heat source model without including the Marangoni effect. Moreover, the generated convective current in the molten pool because of the Marangoni flow modifies temperature found in the melt pool.

5. Numerical modeling in laser surface treatment

Didenko et al. [51–53] studied in detail the laser alloying process of high purity iron with 40 μm Cr electrolytically predeposited on the sample surface. The authors have used the CW CO_2 laser generating TEM10 Gaussian mode with an output power of 2 kW and 2.5 kW focused to the diameter of 3 mm and constant speed of the work table set to 18.4 mm/sec. The process was carried out in an argon atmosphere. For the process modeling, a multi-phase mathematical model of the laser remelting of high purity iron with a pre-deposited chromium layer was used, resulting from solution of the partial differential equations for conservation of energy, mass, and momentum. The FLUENT program was used for numerical modeling of the fluid flow and mass transfer in the molten pool during laser alloying. Finite element mesh used to simulate alloying process was prepared with the GAMBIT program. The numerical results predicted the final composition in the solidified alloy. Didenko et al. [52,53] compared with corresponding experimental results and the agreement they found was good. The non-uniform chromium distribution (the presence of high chromium concentration fields near the solid/liquid interface) is caused by a multi-directional liquid material movement, which is due to the presence of few vortexes in the melted pool. The presence of vortexes in the liquid is caused by the non-uniform energy distribution in the laser beam (TEM10 mode), which directly

http://dx.doi.org/10.5772/62334

influences the mass transport kinetics and gives rise to the final dimension and shape of the melted pool, its microstructure and, consequently, properties of the resolidified material.

Mondal et al. [54] studied Ni-Cr-Mo cladding on mild steel surface using CO_2 laser and process modeling with response surface methodology (RSM). An anti-corrosive powder mixture of Ni, Cr, and Mo with a selected ratio is deposited as a thin layer on the mild steel plate with the help of 3.5 kW CO_2 laser. Experiments were performed according to L_9 Taguchi orthogonal array. The study of the influence of process parameters on responses and process optimization to find the optimal input parameters combination by expecting the improved clad quality was also studied. Based on experimental data, a mathematical model was developed to find the relationship between process input parameter and responses. It was discovered that there is a high degree of approximation between the experimental results and the predicted one. The results of the experiment were extended to develop the regression model using response surface methodology (RSM). Multi-objective optimization was done to find out the optimal parametric setting to achieve desired clad bead dimension with aspect ratio ≤ 15, during laser cladding process. The optimization result showed that at laser power of 1.014 kW, scan speed of work table at 0.475 mm/min, and powder feed rate of 8.807 g/min, both the responses clad height and clad width are optimized at 0.25 mm and 3.85 mm, respectively. From the regression model, scan speed of work table and powder feed rate were the most significant parameters in laser cladding process. It was concluded that the range of these parameters should be selected carefully because the clad quality was very sensitive to these responses. The response surface methodology was found to be effective for the identification of key process parameters and development of significant relationship between the process variables and response.

Kochure and Nandurkar [55] applied the use of the Taguchi method of experimental design with L_9 orthogonal for selection of optimum process parameters of induction hardening of EN8 D steel. Orthogonal arrays L_9, signal to noise ratio, and analysis of variance (ANOVA) were applied to study performance characteristics of induction hardening process. Hardness and case depth were considered as performance characteristics. An analysis of variance (ANOVA) of response variables showed a significant influence on process variable power and heating time. The experimental investigation showed the effects of process parameters such as power, heating time on hardness, and case depth pattern achieved on work piece. The optimum parameters found were 14 kW power and heating time 4 sec, and power is the most influential parameter. Further multiple regression equations were formulated for estimating predicted values of hardness and case depths at various locations such as case depths at outer and inner vertical, top, and center portion of slots for a specified range. The results obtained by regression equations closely co-relate each other, which validate the regression equation developed.

A range of researchers carried out their extensive research work using CO_2 laser to investigate the laser coating performance on corrosion and wear behavior. Kathuria [56] presented a study of laser cladding process in both stationary and scanning beam modes with the laser cladding of satellite six on mild steel and Cr-Ni materials. The effects of the various parameters such as input power, beam interaction time, scanning frequency, and traverse speed were considered. Shepeleva et al. [57] presented a comparison between the laser cladding process in which the

method of direct injection of cladding powder into the melt pool is used and plasma cladding process. They captured optical and SEM photographs of cross-section of clad-substrate interface. It was found that the laser-cladded zone has a smooth interface with the substrate, which prevents stress concentration at the clad-substrate interface during application. They also concluded that the laser-cladded zone, unlike the plasma treated surfaces, is free of micro-cracks and pores. Chryssolouris et al. [58] performed an experimental investigation on laser cladding with aluminum alloy as substrate and copper-based powder as cladding material. The process parameters of their experiments were powder feed rate (g/min), process speed (mm/min), and gas supply (l/h). They observed that the process speed did not affect dilution depth, while increasing powder feed rate might have a negative effect on performance. They concluded that to achieve an optimum clad result, in terms of increased clad depth and minimum alloying zone, powder feed rates should be kept low and process speed should be high. Meng et al. [59] conducted powder laser cladding experiments to improve wear resistance of titanium alloy (Ti-6Al-4V substrate) using NiCoCrAlY powder. The process parameters of this process were laser power (750 W), scanning speed (3–7 mm/s), and laser beam diameter (Φ3 mm). They observed that with high laser scanning speed, thick preplaced powder layer could not be melted completely and the quality of the coating was poor. They concluded that with the preplaced NiCoCrAlY powder, a laser cladding on Ti-6Al-4V surface without cracks and pores could be obtained, and micro-hardness of the surface is two times higher than that before cladding. Davim et al. [60] performed experimental study on geometric form of clad layer. They examined the effect of processing parameters such as laser power, scanning velocity, and powder mass flow rate on clad height, clad width, and depth penetration into the substrate. An analysis of variance (ANOVA) was performed to investigate the influence of processing parameters in the form of single cladding layer and hardness of coating. They also presented a prediction of laser clad geometry for coaxial laser cladding process (6 kW continuous CO_2 laser) through linear multiple regression analysis. They concluded that clad height increased with powder mass flow rate and laser power and decreased with scanning velocity. The depth of penetration increased with laser power and powder mass flow rate. The clad width increased with powder mass flow rate. The present work investigates the parametric effects of laser cladding parameters such as laser power, scan speed, and powder feed rate on performance evaluation parameters, namely clad height and clad width and a process optimization for the selection of optimal parameters combination using response surface methodology (RSM). The result of optimization can be used to set the process parameters at optimum level for the better clad quality during laser cladding operation. The result obtained through RSM technique can also be compared with other optimization method such as genetic algorithm and scatter search approach.

Mondal et al. [61] studied process optimization for laser cladding operation of alloy steel using genetic algorithm and artificial neural network: an investigation on single objective optimization for CO_2 laser cladding process considering clad height (H) and clad width (W) as performance characteristics. The equipment used for laser cladding was a 3.5 kW continuous wave CO_2 Laser Rapid Manufacturing (LRM) system. The LRM set-up consists of a high power laser system integrated with the beam delivery system, powder feeding system, and job/beam manipulation system. The key process parameters were laser power, scan speed, and powder

http://dx.doi.org/10.5772/62334

feed rate. First, numerous single tracks were deposited at various machining conditions to obtain continuous and uniform tracks, which facilitated to determine the range of process parameters for control levels in Taguchi method. Then the actual experiments were performed as per the L_9 Taguchi orthogonal array. This optimization of multiple quality characteristics has been done using genetic algorithm (GA) approach. The aim of this work was to predict the performance characteristics (*H* and *W*) at optimized condition by applying back propagation method of artificial neural network (ANN). The essential input process parameters are identified as laser power, scan speed of work table, and powder feed rate. To validate the predicted result, an experiment as confirmatory test was carried out at the optimized cladding condition. It was observed that the confirmatory experimental result was showing a good agreement with the predicted one. It has also been found that the optimum condition of the cladding parameters for multi-performance characteristics varies with the different combinations of weighting factors.

Zuljan and Uran [62] studied the optimization of the laser wire cladding of tool steels using factor analysis. The aim was to establish reliable correlations between the input parameters and the parameters of laser wire cladding quality used in optimization. Using a Nd:YAG laser as the energy source, laser wire cladding was carried out on the seven most frequently used tool steels (1.2311, 1.2312, 1.2343, 1.2344, 1.2767, 1.2379, and 1.2550). The quality of a laser wire clad-weld was defined by their geometrical characteristics, mechanical properties, and minimum internal stresses in the area of the laser wire clad-weld. The importance of the general correlations between the laser wire cladding parameters was determined by means of a statistical factor analysis, which provides factor loadings with the variables. The laser wire cladding analysis was carried out through the purposeful selection of control parameters and monitoring of the laser wire clad-weld quality parameters. The results obtained and the laser wire cladding research procedure used provide a suitable tool for attaining the desired laser wire clad-weld quality and can be used by laser wire cladding designers and technologists.

Ermurat et al. [63] studied process parameters investigation of a laser-generated single clad for minimum size using design of experiments. The aim of the study was to investigate the effect of four important process parameters (i.e., laser focal distance, travel speed, feeding gas flow rate, and standoff distance) on the size of single clad geometry created by coaxial nozzle-based powder deposition by high power laser. Design of experiments (DOE) and statistical analysis methods were both used to find optimum parameter combinations to get minimum-sized clad, that is, clad width and clad height. Factorial experiment arrays were used to design parameter combinations for creating experimental runs. This procedure was somehow complicated in understanding the effects of the selected problem parameters on the outcome. Therefore, DOE methodologies were utilized so that the operation can be better modeled/understood and automated for real life applications. The study also gives future direction for research based on the presented results. Taguchi optimization methodology was used to find out optimum parameter levels to get minimum sized clad geometry. Response surface method was used to investigate the non-linearity among parameters, and variance analysis was used to assess the effectiveness level of each problem parameters. The overall results showed that wisely selected four problem parameters had the most prominent effects on the final clad

geometry. Minimum clad size was achieved at higher levels of gas flow rate, travel speed, and standoff distance and at minimum spot size level of the laser focal distance.

Influence of the process parameters was experimented to be able to produce minimum-sized clads created by laser-assisted direct metal part fabrication system using DOE and statistical analysis methods. Several process parameters affect the size of the clad geometry. Laser focal distance, standoff distance, gas flow rate, and travel speed were investigated, and the conclusions can be written as follow: Laser energy intensity is varying at different levels of laser focal distance because the size of the laser spot is changing at each level; results changing of the intensity of the penetrated energy to the substrate. Travel speed relates to the interaction time between laser spot and substrate material, which affects the clad size since dominating the size of the molten pool. Higher travel speeds shorten the interaction time and make the clad size small. Clad size reduces with the increase of the standoff distance. The effect of the standoff distance should be lowered as much as possible to build complex part geometry in good condition. The high level of feeding gas flow rate, minimum sized geometry was achieved because of reducing the powder-laser beam interaction time by increasing the powder particle speed. In addition, there is a powerful relation between standoff distance and gas flow rate. Standoff distance and feeding gas flow rate are the parameters that dominate the shape of the particle flow including particle speed. On top of that, shape of the laser beam waist has a connection about rate of the intensity of each particle moving through the beam of laser.

Mondal et al. [64] studied the application of artificial neural network for the prediction of laser cladding process characteristics at Taguchi-based optimized condition. An investigation on the optimization of multiple performance characteristics during CO_2 laser cladding process considering clad width and clad depth as performance characteristics has been presented. This optimization for multiple quality characteristics has been done using Taguchi's quality loss function. In the present work, a number of experiments have been performed to establish the interrelationship between process variables and response variables using the back propagation method of ANN. The essential input process parameters were identified as laser power, scan speed of work table, and powder feed rate. Moreover, the analysis of variance was also employed to determine the contribution of each control parameter on clad bead quality. To validate the predicted result, an experiment as confirmatory test was carried out at the optimized cladding condition. It was observed that the confirmatory experimental result was showing a good agreement with the predicted one. However, it has been found that the optimum condition of the cladding parameters for multi-performance characteristics varies with the different combinations of weighting factors.

Mondal et al. [65] studied the application of Taguchi-based gray relational analysis for evaluating the optimal laser cladding parameters for AISI1040 steel plane surface. The effect of various laser cladding process parameters such as laser power, scan speed, and powder feed rate on clad bead quality characteristics (or clad bead geometry) for AISI 1040 steel substrate have been studied by performing a number of experiments with L_9 orthogonal array. To find the process parametric setting for best quality clad bead based on experimental results, a multi-response optimization technique using gray relational analysis (GRA) was used. The GRA was applied on laser cladding process to find out the grey relational grade for each experiment. On

http://dx.doi.org/10.5772/62334

optimization, power of 1.25 kW, scan speed of 0.8 m/min, and a powder feed rate of 11 gm/min had been found to be the best parametric setting for laser cladding operation of AISI 1040 steel substrate. Moreover, the analysis of variance was also performed to determine the contribution of each control factor on the clad quality characteristics. Finally, to ensure the robustness of GRA, a confirmatory test was performed at selected optimal parametric setting. An expression of gray relational analysis that directly integrates the multiple performance characteristics (i.e., laser power, scan speed, and powder feed rate) into a single performance characteristic is called gray relational grade. Therefore optimization of the complicated multiple performance characteristics can be greatly simplified to a single objective optimization problem through this approach. It was found that the performance characteristics of the laser cladding process such as clad height, clad width, and clad depth were improved together using this methodology. Furthermore, from the results of ANOVA, the contribution of each cladding factor on the cladding quality characteristics in decreasing order were laser power, scan speed of work table, and powder feed rate. Finally, the confirmation tests had ensured the robustness of the optimal combination of laser cladding process for AISI 1040 steel surface.

Babu et al. [66] carried out a systematic investigation on laser transformation hardening (LTH) process on high-strength low-alloy medium carbon steel using design of experiments (DOE). The effect of input process parameters such as laser power, travel speed over the response hardened width (HW), hardened depth (HD), and hardened area (HA) were analyzed. The experimental trials were conducted based on the design matrix obtained from the 3k full factorial design (FFD) using a 2 kW continuous wave Nd:YAG laser power system. A quadratic regression model was developed to predict the responses using response surface methodology (RSM). Based on the developed mathematical models, the direct and interaction effects of the process parameters on LTH were investigated. The optimal hardening conditions were identified to maximize the HW and minimize the HD and HA. The results of the validation test showed that the experimental values quite satisfactorily agreed with the predicted values of the mathematical models and hence, the models can predict the response adequately.

6. 3D-simulation of laser molten pool

Yang et al. [67] reported that to study the mechanism of convection in theory, 3D computer simulation of convection and heat transfer in laser molten pool is needed. The main physical process in laser molten pool requires some of the laser beams to be absorbed while the rest is reflected. If the threshold is exceeded by the heat absorbed, the molten pool will be developed. In stationary melting, molten pool shape and absorbability are constant. The buoyancy force and the surface tension gradient are the two driving forces for fluid flow in laser melt pool.

The surface tension gradient and the buoyancy force are defined by the following equations:

$$\frac{\partial \gamma}{\partial x} = \frac{\partial T}{\partial x} \cdot \frac{\partial \gamma}{\partial T} \tag{5}$$

$$F_b = -\rho\beta\Delta T_g \tag{6}$$

While the governing equations can be written as [68]:

Continuity:

$$\frac{\partial\rho}{\partial t} + \rho\nabla.\vec{V} = 0 \tag{7}$$

Momentum equation:

$$\rho[\frac{\partial\vec{V}}{\partial t} + (\vec{V}.\nabla)\vec{V}] = \mu\nabla^2\vec{V} - \nabla P + F_b \tag{8}$$

Energy equation:

$$\frac{\partial\vec{T}}{\partial t} + (\vec{V}.\nabla)T = \alpha\nabla^2 T \tag{9}$$

Where $\vec{V} = u\vec{i} + v\vec{j} + w\vec{k}$

V = Total velocity of fluid, u, v, and w are components of V in x, y, and z direction, respectively.

μ = Viscosity

γ = Surface tension

β = Volumetric thermal expansion coefficient

g = gravitational acceleration

T = Temperature

P = Pressure

ρ = Mass density

α = Thermal diffusivity

Yang et al. [67] compared the effects of surface tension gradient and buoyancy force and their fluid fields in laser molten pool with computer simulation. It was discovered that in the center of molten pool, the fluid flow direction was from the bottom to the top. Likewise, on the surface of the molten pool, the fluid flow direction was from the center to the edge and in the interface of solid-liquid, the fluid flow direction was from top to bottom thereby producing a circular flow. As $\frac{\partial\gamma}{\partial T}$ liquid iron is negative, $\frac{\partial\gamma}{\partial x}$ in the pool center is lower than that in the pool edge;

http://dx.doi.org/10.5772/62334

therefore, liquid metal is drawn from center to edge. The Reynolds number (Re) was about 1200 (<critical Re=2000), which indicates a planar flow. The convection field pattern because of buoyancy force and surface tension are similar. This means they have the same flow direction from bottom to top in the pool center. The authors concluded that convection in laser molten pool is mainly induced by surface tension gradient. Finally, the authors concluded that there was a strong convection and heat transfer in laser molten pool. There are left and right flow cycles symmetrical to the plane center, which was perpendicular to the moving direction of laser beam. Convention and heat transfer caused the laser molten pool widen. The simulated results agreed with experimental results.

7. Conclusion

The following conclusions can be deduced:

- The application and effectiveness of LSA are highly dependent and sensitive to small changes in process parameters, and these process parameters play a significant role in the quality of the alloyed layer.
- When metal foam is in the phase changing environment, the heat transfer process is conduction dominated, irrespective of the heat source pulse width.
- Convection in laser molten pool is mainly induced by surface tension gradient. Also, the buoyancy force and the surface tension gradient are the two driving forces for fluid flow in laser melt pool.
- A little imbalance in the process parameters can result in large variations in the geometry, microstructure, and properties of the alloyed zone.
- Careful selection and control of process parameters through an optimization process are required to establish an appropriate laser power-scan speed combination for achieving defect-free alloyed layers.

Author details

Olawale S. Fatoba[1*], Patricia A.I. Popoola[1*], Sisa L. Pityana[1,2] and Olanrewaju S. Adesina[1]

*Address all correspondence to: fatobaolawale@yahoo.com; popoolaapi@tut.ac.za

1 Department of Chemical, Metallurgical and Materials Engineering, Tshwane University of Technology, Pretoria, South Africa

2 Centre for Scientific and Industrial Research-National Laser Centre, Pretoria, South Africa

References

[1] Kelbassa, I. (2011). Laser surface treatment and additive manufacturing: Basics and application examples.

[2] Steen, W.M., Mazumdar, J. (2010). Laser material processing. 4th edition, Springer-Verlag London Ltd., London.

[3] Lo, K.H., Cheng, F.T., Kwok, C.T., Man, H.C. (2003). Improvement of cavitation erosion resistance of AISI 316 stainless steel by laser surface alloying using fine WC powder. Surface and Coatings Technology. 165: 258–267.

[4] Oberlander, B.C., Lugscheider, E. (1992). Comparison of properties of coatings produced by laser cladding and conventional methods. Materials Science and Technology. 8: 657–665.

[5] Li, C., Wang, W., Han, B. (2011). Microstructure, hardness and stress in melted zone of 42CrMo steel by wide-band laser surface melting. Optics and Lasers in Engineering. 49: 530–535.

[6] Wirth, P. (2004). Introduction to industrial laser materials processing. Rofin, Germany.

[7] Labuschagne, K. (2006). Investigative study of martensite formation in laser transformation hardened steels. M-Tech. dissertation, Pretoria, Tshwane University of Technology.

[8] Steen, W.M., Powell, J. (1981). Laser surface treatment. Materials in Engineering (Surrey, England). 2(3): 157–162.

[9] Steen, W.M., Mazumdar, J. (2010). Laser material processing. 4th edition, Springer-Verlag London Ltd., London.

[10] Steen, W.M. (1998). Laser material processing. 2nd edition, Springer-Verlag London Ltd., London.

[11] Kusinki, J., Kac, S., Kopia, A., Radziswewska, A., Rozmus-Gornikowska, M., Major, B., Major, L., Marckar, J., Lisiecki, A. (2012). Laser modification of materials surface layer-review paper. Bulleting of the Polish Academy of Sciences. 60(4): 711–728.

[12] Mondal, A.K., Kumar, S., Blawert, C., Dahotre, N.B. (2008). Effect of laser surface treatment on corrosion and wear resistance of ACM720 Mg alloy. Surface and Coatings Technology. 202: 3187–3198.

[13] Kwok, C.T., Cheng, F.T., Man, H.C. (2006). Cavitation erosion and corrosion behaviour of laser –aluminized mild steel. Surface and Coatings Technology. 200: 3544–3552.

[14] Dobrzanski, L.A., Piec, M., Bonek, M., Jonda, E., Klimpel, A. (2007). Mechanical and tribological properties of the laser alloyed surface coatings. Journal of Achievements in Materials and Manufacturing Engineering. 20(1–2): 235–238.

[15] Fagagnolo, J.B., Rodrigues, A.V., Lima, M.S.F., Amigo, V., Caram, R. (2013). A novel proposal to manipulate the properties of titanium parts by laser alloying. Scripta Materialia. 68: 471–474.

[16] Brytan, Z., Bonek, M., Dobrzanski, L.A. (2010). Microstructure and properties of laser surface alloyed PM austenitic stainless steel. Journal of Achievements in Materials and Manufacturing Engineering. 40(1): 70–79.

[17] Li, J., Chen, C., Zhang, C. (2011). Phase constituents and microstructure of Ti_3Al/Fe_3Al + TiN/TiB_2 composite coating on titanium alloy. Surface Review and Letters. 18: 103–108.

[18] Kwok, C.T., Lo, K.H., Cheng, F.T., Man, H.C. (2003). Effect of processing conditions on the corrosion performance of laser surfaced melted AISI 440C martensitic stainless steel. Surface and Coatings Technology. 166: 221–230.

[19] Adebiyi, D.I., Popoola, A.P.I., Pityana, S.L. (2014). Microstructural evolution at the overlap zones of 12Cr martensitic stainless steel laser alloyed with TiC. Optics and Laser Technology. 61: 15–23.

[20] Wei, L., Huijun, Y., Chuanzhong, C., Diangang, W., Fei, W. (2013). Microstructures of hard coatings deposited on titanium alloys by laser alloying technique. Surface Review and Letters. 20: 1–6.

[21] Yakovlev, A., Bertrand, P., Smurov, I. (2004). Laser cladding of wear resistant metal matrix composite coatings. Thin Solid Films. 453: 133–138.

[22] Poulon-Quintina, A., Watanabe, I., Bertranda, C., Watanabe, E. (2012). Microstructure and mechanical properties of surface treated cast titanium with Nd:YAG laser. Dental Materials. 28: 945–951.

[23] Zhou, R., Sun, G.F., Chen, K.K., Tong, Y.Q. (2014). Effect of tempering on microstructure mechanical properties of cast iron rolls laser alloyed with C-B-W-Cr. Proceedings of the Global Conference on Polymer and Composite Materials.

[24] Sugioka, K., Cheng, Y. (2014). Ultrafast lasers-reliable tools for advanced materials processing. Light: Science & Applications. 3–30

[25] Toyserkani, E., Khajepour, A., Corbin, S. (2005). Laser cladding. CRC press, London.

[26] Svelto, O. (1998). Principles of lasers. 4th edition, Plenum Press, New York.

[27] Steen, W.M. (2003). Laser material processing. 3rd edition, Springer-Verlag London Ltd., London.

[28] Berkmanns, J., Faerber, M. (2010). Laser basics, BOC. Available from: https://boc.com.au/boc_sp/downloads/gas_brochures/BOC_216121_Laser%20Basics_v7.pdf.

[29] Callen, H.B. (1960). Thermodynamics, 31–58.

[30] Holman, J.P. (1989a). Heat transfer, SI Metric edition, 2–6.

[31] Müller, I. (1985a). Thermodynamics (Interaction of Mechanics and Mathematics Series), 1–3.

[32] Müller, I. (1985b). Thermodynamics (Interaction of Mechanics and Mathematics Series), 47–68.

[33] Holman, J.P. (1989b). Heat transfer, SI Metric edition, 10–15.

[34] Kwok, C.T., Cheng, F.T., Man, H.C. (2006). Cavitation erosion and corrosion behaviour of laser – aluminized mild steel. Surface and Coatings Technology. 200: 3544–3552.

[35] Dobrzanski, L.A., Piec, M., Bonek, M., Jonda, E., Klimpel, A. (2007). Mechanical and tribological properties of the laser alloyed surface coatings. Journal of Achievements in Materials and Manufacturing Engineering. 20(1–2): 235–238.

[36] Chande, T., Mazumder, J. (1983). Composition control in laser surface alloying. Metallurgical Transactions B. 14B: 181.

[37] Pawlowski, L. (1999). Thick laser coatings: A review. Journal of Thermal Spray Technology. 8(2): 279–295.

[38] Yang, L.X., Peng, X.P., Wang, B.X. (2001). Numerical modelling and experimental investigation on the characteristics of molten pool during laser processing. International Journal of Heat and Mass Transfer. 44: 4465–4473.

[39] Sarkar, S., Raj, P.M., Chakraborty, S., Dutta, P. (2002). Three dimensional computational modeling of momentum, heat and mass transfer in a laser surface alloying process. Numerical Heat Transfer Part A. 42: 307–326.

[40] Raj, P.M., Sarkar, S., Chakraborty, S., Dutta, P. (2001). Three dimensional computational modeling of momentum, heat and mass transfer in laser surface alloying with distributed melting of alloying element. International Journal of Numerical Methods for Heat & Fluid Flow. 11(6): 576–599.

[41] Chung, H., Das, S. (2004). Numerical modeling of scanning laser- induced melting, vaporization and resolidification in metals subjected to step heat flux input. International Journal of Heat and Mass Transfer. 47: 4153–4164.

[42] Li, J.F., Li, L., Stott, F.H. (2004). Comparison of volumetric and surface heating surfaces in the modeling of laser melting of ceramic materials. International Journal of Heat and Mass Transfer. 47: 1159–1174.

[43] Safdar, S., Li, L., Sheikh, M.A. (2007). Numerical analysis of the effects of non-conventional laser beam geometries during laser melting of metallic materials. Journal of Physics D: Applied Physics. 40: 593–603.

[44] Uglov, A.A., Smurov, I.Y., Taguirov, K.I., Guskov, A.G. (1992). Simulation of unsteady-state thermocapillary mass transfer for laser doping of metals. International Journal of Heat and Mass Transfer. 35(4): 783–793.

[45] Smurov, I., Covelli, L., Tagirov, K., Aksenov, L. (1992). Peculiarities of pulse laser alloying: Influence of spatial distribution of the beam. Journal of Applied Physics. 71(7): 3147–3158.

[46] Yuan, Z., Mukai, K., Huang, W. (2002). Surface tension and its temperature coefficient of molten silicon at different oxygen potentials. Langmuir. 18: 2054–2062.

[47] He, X., Fuerschbach, P.W., DebRoy, T. (2003). Heat transfer and fluid flow during laser spot welding of 304 stainless steel. Journal of Physics D: Applied Physics. 36: 1388–1398.

[48] Xichen, Y. (1990). Study on wide-band pattern of laser heat treatment [J]. Chinese Journal of Lasers. 17(4): 229–235.

[49] Konrad, C., Zhang, Y., Shi, Y. (2007). Melting and resolidification of a subcooled metal powder particle subjected to nanosecond laser heating. International Journal of Heat and Mass Transfer. 50: 2236–2245.

[50] Bin-Mansoor, S., Yilbas, B.S. (2006). Laser pulse heating of steel surface: Consideration of phase change process. Numerical Heat Transfer, Part A. 50(8): 787–807.

[51] Didenko, T. (2006). Laser surface melting – modelling and experimental verification of the melted zone shape and size, and chemical homogeneity. PhD Thesis, AGH University of Science and Technology, Kraków, 2006 (in Polish).

[52] Didenko, T., Kusinski, J., Kusinski, G. (2006). Multiphase model of heat and mass transport during laser alloying of iron with electrodeposited chromium layer. Proceedings of Multiscale and Functionally Graded Materials Conference. 1: 640–646.

[53] Didenko, T., Siwek, A., Kusinski, J. (2004). Numerical modelling of the laser alloying process. Proceedings of XI Conference: Informatics in Metals Technology. 1: 179–186.

[54] Mondal, S., Asish, B., Pradip, K. (2011). Ni-Cr-Mo cladding on mild steel surface using CO_2 laser and process modeling with response surface methodology. International Journal of Engineering Science and Technology. 3: 6805–6816.

[55] Kochure, P.G., Nandurkar, K.N. (2012). Taguchi method and ANOVA: An approach for selection of process parameters of induction hardening of EN8 D steel. International Journal of Advance Research in Science, Engineering and Technology. 1(2): 22–27.

[56] Kathuria, Y.P. (1997). Laser-cladding process: A study using stationary and scanning CO_2 laser beams. Surface & Coatings Technology. 97: 442–447.

[57] Shepeleva, L., Medres, B., Kaplan, W.D., Bamberger, M., Weisheit, A. (2000). Laser cladding of turbine blades. Surface & Coatings Technology. 125: 45–48.

[58] Chryssolouris, G., Zannis, S., Tsirbas, K., Lalas, C. (2002). An experimental investigation of laser cladding. CIRP Annals: Manufacturing Technology. 51(1): 145–148.

[59] Meng, Q., Geng, L., Ni, D. (2005). Laser cladding NiCoCrAlY coating on Ti-6Al-4V. Materials Letters. 59(22): 2774–2777.

[60] Davim, J.P., Oliveira, C., Cardoso, A. (2006). Laser cladding: An experimental study of geometric form and hardness of coating using statistical analysis. Proceedings of the Institute of Mechanical Engineers, Part B: Journal of Engineering Manufacture. 220(9): 1549–1554.

[61] Mondal, S., Tudu, B., Asish, B., Pradip, K. (2012). Process optimization for laser cladding operation of alloy steel using genetic algorithm and artificial neural network. International Journal of Computational Engineering Research. 2(1): 18–24.

[62] Zuljan, D., Uran, M. (2010). Optimization of the laser wire cladding of tool steels using factor analysis. Lasers in Engineering. 20: 21–38.

[63] Ermurat, M., Arslan, M.A., Erzincanli, F., Uzman, I. (2013). Process parameters investigation of a laser-generated single clad for minimum size using design of experiments. Rapid Prototyping Journal. 19(6): 452–462.

[64] Mondal, S., Asish, B., Pradip, K. (2014). Application of artificial neural network for the prediction of laser cladding process characteristics at Taguchi-based optimized condition. International Journal of Advanced Manufacturing Technology. 70: 2151–2158.

[65] Mondal, S., Paul, C.P., Kukreja, L.M. (2013). Application of Taguchi-based gray relational analysis for evaluating the optimal laser cladding parameters for AISI 1040 steel plane surface. International Journal of Advanced Manufacturing Technology. 66: 91–96.

[66] Babu, P.D., Buvanashekaran, G., Balasubramanian, K.R. (2013). Experimental investigation of laser transformation hardening of low alloy steel using response surface methodology. International Journal of Advanced Manufacturing Technology. 67: 1883–1897.

[67] Yang, B., Yang, X.C., Lei, J.B., Wang, Y.S. (2013). Computer simulation of physical transfer process in laser molten pool. Applied Mechanics and Materials. 341–342: 324–328.

[68] Brent, A.D., Voller, V.R., Reid, K.J. (1988). The enthalpy-porosity technique for modeling convection diffusion phase change: Application to the melting of a pure metal. Numerical Heat Transfer. 13: 297–318.